Optimal Tuning of PID Controller for Boost Converter using Meta-Heuristic Algorithm for Renewable Energy Applications

Muhammad Hamza Zafar
Department of Electrical Engineering
Capital University of Science and Technology
Islamabad, Pakistan
hamzauetms@gmail.com

Majad Mansoor
Department of Automation
University of Science and Technology of China
Hefei, China
majad@mail.ustc.edu.cn

Noman Mujeeb Khan
Department of Electrical Engineering
Capital University of Science and Technology
Islamabad, Pakistan
naumanmujeebk@gmail.com

Filippo Sanfilippo
Department of Engineering Sciences
University of Agder (UiA)
Grimstad, Norway
Department of Software Engineering
Kaunas University of Technology
Kaunas, Lithuania
filippo.sanfilippo@uia.no

***Abstract*—The Dynamic Levy Flight Chimp optimisation (DLFC) method is used in this study to optimise the Proportional-Integral-Derivative (PID) Controller for the Boost converter. As a possible application, the tuned PID controller is utilised to adjust voltages in the use of renewable power sources. The maximum power point tracking control approach based on machine learning (ML) is used to anticipate the reference voltages for the solar system based on the irradiance and the ambient temperature. The tuned PID controller uses this reference signal to regulate the maximum power point (MPP) voltages. To fine-tune the PID controller, comparisons are done with grey wolf optimiser (GWO), Harris hawk optimisation algorithms (HHO), and particle swarm optimisation (PSO) algorithms. The tuned PID controller has fewer oscillations and requires little tracking time to adapt to changing load and environment conditions. Additionally, statistical analysis, such as Mean Absolute Error (MAE) and Root Mean Square Error (RMSE) between the reference voltage and the output voltage, is presented. Since the DLFC tuned PID controller performs better than HHO, GWO, and PSO in terms of RMSE and MAE, it may be a promising way for optimising PID controller tuning for boost converters in photovoltaic (PV) system applications.**

***Index Terms*—Proportional Integral Derivative (PID), Swarm Intelligence (SI), Renewable Energy (RE), Statistical Analysis.**

I. Introduction

Since the 1950s, the vast majority of controllers on the market have been Proportional-Integral-Derivative (PID) controllers. They have found widespread use in a variety of control applications involving electrical power circuits and systems. PID controllers work to minimise the gap that exists between the actual outputs of a plant and the outputs that are intended. Both the steady state and the transient responses may be enhanced by using this method. PIDs are currently being researched for a variety of uses, including academic and industrial settings, and a variety of alternative structures are being studied for them. One of the most used application of PID controllers are in Boost converters that are used with photovoltaic systems [1].

In distributed solar power generation systems, boost converters are frequently utilised to raise the low module voltage to the greater load voltage. An example of a conventional photovoltaic (PV) power generating system that is connected to the grid is shown in Fig. 1. The output can be utilised to either directly supply electricity to the load or link to the electricity network. A Boost circuit's main functions are voltage enhancing, voltage control, electrical isolation, and current fluctuation reduction. After the power has been converted, the output voltage of the solar cell has to be changed to a steady value to facilitate the functioning of the power inverter. This is accomplished via the process of voltage boosting [2]. Electrical isolation refers to the process of isolating the photovoltaic panel from the inverter in order to increase the degree of safety and prevent disturbance. The working performance of solar panels may be improved while also increasing their lifespan if the current fluctuation is lowered. For its straightforward algorithm and straightforward implementation, the PID controller is used to manage the switching on and off of the power switch for the Boost circuit in order to produce the effect of output voltage stability [3].

However, if the process variable is very dynamic, it is difficult to select the appropriate PID controller parameters using only one's previous experience. Furthermore, using fixed controller parameters is unable to cause the controlled object to designing appropriate performances under an array of diverse operational conditions [4].

PID controllers are fairly common, however one of their main drawbacks is that they require tuning in order to perform properly. PID controllers may be tuned using a wide range of methodologies, from conventional methods that rely on mathematical simulation and control of dynamic response to methods relying on meta-heuristic optimisation algorithms to determine the PID controller's ideal model parameters [5]. PID controllers are used in a wide variety of applications. In conjunction with Fuzzy logic it provides a complex control requiring costly hardware implementation [6]. Many of the optimisation algorithms that have been developed up to this point have taken their cues from the collective behaviour of live creatures when it comes to the quest for food or the betterment of their breed [7].

It is essential to achieve optimal tuning of DC-DC converters because of the influence these devices have on renewable energy systems [8]. When it comes to adjusting DC-DC converters, one of the most effective types of procedures is intelligent optimisation methods [9].

Conventional PID tuning techniques i.e., trial and error method, Ziegler-Nichols, Cohen-Coon Method have low efficiency due to high settling time and high oscillations at the set point. Intelligent tuning techniques i.e. meta-heuristic based tuning is a viable solution for the tuning of PID controllers for Boost converters. In this paper, Dynamic Levy Flight Chimp Optimisation (DLFCO) based PID tuning method is proposed. This method is based upon a semi hybrid model that makes use of data driven approach to investigate the optimum gains of standard PID control. It allows for a flexible utility of Maximum Power Point Tracking (MPPT) control application to the PV system under various operating conditions. This technique increases the efficiency of the system due to less settling time and low oscillations at the maximum power point.

This paper is organised as follows: Section 1 is the Introduction, Boost Converter modelling is explained in Section 2, Section 3 includes the proposed technique, results and corresponding discussion are added in Section 4, Section 5 includes the conclusion of the paper.

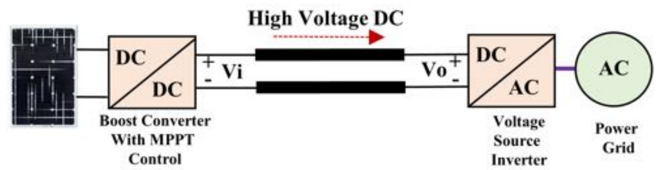

Fig. 1. Typical PV Power Generation System

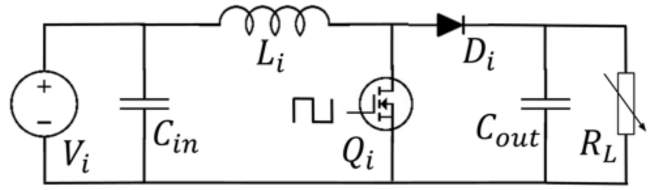

Fig. 2. Schematic of a Boost Converter

II. Boost Converter Modelling

The boost converter mathematical model is initially described in this part, followed by an explanation of the boost converter's closed-loop control using a PID controller.

A. Boost Converter

Fig. 2 shows a conventional Boost converter arrangement. For modelling, the high frequency averaging approach is applied. This technique is based on aggregating the shifting element parameters and utilising a controlled source instead of nonlinear switching devices [10] to construct an equivalent circuit, and then the transfer function of a Boost converter is derived using the small signal method, as shown below:

$$G_v(s) = \frac{(V_i((1-D)^2R - sL))}{((1-D)^2((1-D)^2R + sL + s^2RLC))} \quad (1)$$

where, G_v is the transfer function, V_i is the input voltage, D is the duty cycle, Load is represented by R, L and C represents the inductor and capacitor used in converter, respectively.

B. PID Controller for Boost Converter

In order for the boost converter to respond to any disruptions and variations in rated voltage and load, it requires a PID controller. The mathematical equation u(t), which symbolises the PID controller, is shown in Eq. 2. The controller controls the error signal e(t), which is the difference between the reference voltage and the converter output voltage, in a proportional, integrated, and derived way:

$$u(t) = K_p[e(t) + \frac{1}{T_i}\int_0^t e(t)dt + \frac{T_d de(t)}{dt}] \quad (2)$$

where K_p is proportional constant, T_i is the integration time constant, and d_T is the derivation time constant. Finding proportional, integration and derivative action values for a PID controller that minimise the value of the error signal is the goal of setting a PID controller. Such operations can be described as

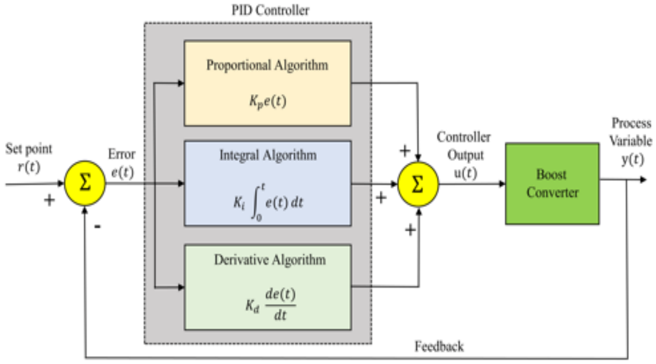

Fig. 3. Close Loop Control of a Boost Converter.

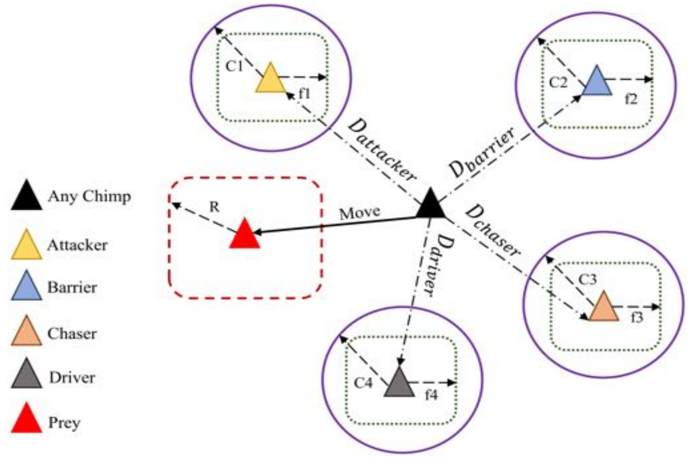

Fig. 4. Structure of Chimp Optimisation Algorithm to solve optimisation problems

the gain constants proportional K_p, integral K_i, and derivative K_d defined in Eq. 3-5.

$$K_p = k \tag{3}$$

$$K_i = K_p/T_i \tag{4}$$

$$K_d = K_p T_d \tag{5}$$

where k denotes the proportional gain constant K_p, K_i, and K_d are the PID controller's integrative and derivative gain constants. The close loop control of boost converter with PID control is shown in Fig. 3.

III. Proposed Technique

In this section, the mathematical model of Dynamic Levy Flight Chimp optimisation (DLFCO) is explained and used to tune the PID gains for the Boost converter. This tuned PID based Boost converter is adopted for the implementation of the MPPT control technique for PV systems.

A. *Chimp optimisation Algorithm (CHoA)*

The ChOA is a computational framework influenced by how chimps hunt in their colony. The paradigm of the algorithm can be investigated subsequently as a distinct research in terms of the novelty of the concept, however we do not assert that the procedures are mathematically unique. Some similarities may occur due to the availability of several techniques and the limitations of updating rules. There are four types of members in a chimpanzee community: drivers, chasers, barriers, and attackers. Each individual has their own special abilities, which are necessary for the group to be successful at hunting. [11]. Generally speaking, the act of hunting that chimpanzees engage in can be broken down into two primary phases: the first is called Exploration and it involves driving, blocking, and pursuing the prey, and the second is called Exploitation and it involves attacking the prey. The structure of ChOA algorithm is shown in 5. The driving and chasing behaviours of the first two roles in group hunting are mathematically characterised as follows:

$$d = |c \cdot Z_{prey}(t) - m \cdot Z_{chimp}(t)| \tag{6}$$

$$Z_{chimp}(t+1) = Z_{prey}(t) - a \cdot d \tag{7}$$

where the locations of the prey and chimpanzees are represented by the matrices Z_{prey} and Z_{chimp}, respectively. The variable t represents the current iteration, and the vectors a, m, and c are given by the equations:

$$a = 2 \cdot f \cdot r_1 - a \tag{8}$$

$$c = 2 \cdot r_2 \tag{9}$$

$$m = chaotic_{value} \tag{10}$$

The function f is non-linearly decreased over a range of iterations from 2 to 0. The values $r1$ and $r2$ are random numbers between 0 and 1. The chaotic value m represents the reproductive impulses of agents using different chaotic sequences. During the exploitation phase, the attacker chimpanzee takes the lead, with the other members sometimes participating in the hunt. It is not possible to accurately determine the exact location of the ideal prey, so the available data is used to mathematically model hunting behavior. The most effective agents are the initial attacker, driver, barrier, and chaser, and the other members should adjust their positions based on these four agents. The rule for adjusting positions is shown in the following equations:

$$d_{Atck} = |c_1 \cdot Z_{Atck} - m_1 \cdot x| \tag{11}$$

$$d_{Barr} = |c_2 \cdot Z_{Barr} - m_2 \cdot x| \tag{12}$$

$$d_{Chsr} = |c_3 \cdot Z_{Chsr} - m_3 \cdot x| \tag{13}$$

$$d_{Dver} = |c_4 \cdot Z_{Dver} - m_4 \cdot x| \tag{14}$$

$$X_1 = Z_{Atck} - a_1 \cdot d_{Atck} \tag{15}$$

$$X_2 = Z_{Barr} - a_2 \cdot d_{Barr} \tag{16}$$

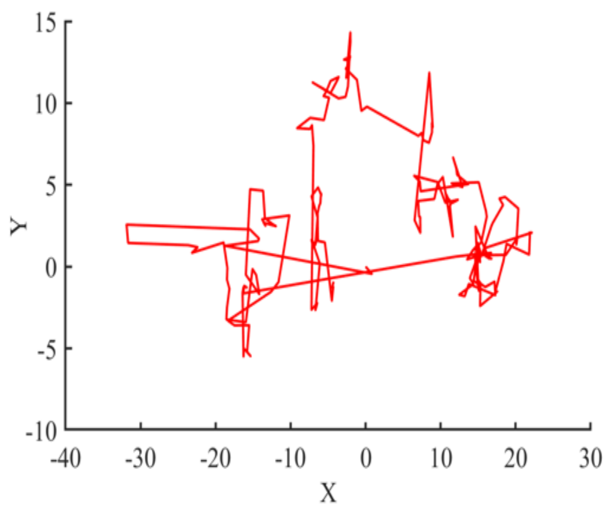

Fig. 5. Levy Flight Movement

$$X_3 = Z_{Chsr} - a_3 \cdot d_{chsr} \quad (17)$$

$$X_4 = Z_{Dver} - a_4 \cdot d_{Dver} \quad (18)$$

$$x(t+1) = \frac{(x_1 + x_2 + x_3 + x_4)}{4} \quad (19)$$

The chaotic behavior of agents during the final stage of hunting, represented by m, is intended to help them acquire more food and increase their chances of receiving social favors such as grooming or mating.

B. Levy Flight

When the probability distribution of a process's collection of variables matches that of each individual variable, the process is said to be stable [12]. The sum of the Gaussian parameters and the Distribution function make up the robust Gaussian process. It is renowned for being stable. However, the Levy probability distribution is more stable than the Gaussian process since it has an infinite second moment. [13]. This probability distribution is defined as follows:

$$L_(al, lem)(x) = 1/\int_0^t e^(- lem \cdot rou^{al})cos(px)dp \quad (20)$$

As demonstrated in Eq. 20, the Levy probability has two factors, namely alpha, and lembda and is also symmetric with respect to x = 0. Where is the scaling factor such that lembda $>$ 0 and is between (0, 2). The parameter regulates the distribution's topology to provide different probability density forms, especially towards the tail.

C. Fusion of CHoA with Levy Flight

The conventional ChOA changes its agents toward the prey according to where the driver, chaser, barrier, and attacker are placed (optimal position). The exploring agents of ChOA are, however, occasionally nevertheless vulnerable to local minima that stagnate. Due to this, the issue of embryonic convergence can still exist. The shift between the exploration and exploitation stages is not always easy to achieve with the standard ChOA. To cope with the issues that were previously found, LF is used in this section. The worldwide search can be sped up by using the DLFCO's deeper searching patterns. Stasis can be lessened with the use of this mixture. Additionally, DLFCO's agents' quality has to improve with each iteration. As a result, the chimp's position update of DLFCO is defined as Eq. 21 and Eq. 22 rather than Eq. 19. Therefore, Eq. 21 and 22 are shown below used for updation of particle position.

$$X_{chimp} = \frac{x_1 + x_2 + x_3 + x_4}{4} + levy(W_1) \cdot rand() \quad (21)$$

$$X_{chimp} = \frac{x_1 + x_2 + x_3 + x_4}{4} + levy(W_2) \cdot rand() \quad (22)$$

D. PID Tuning using DLFCO

An intelligent strategy is employed in this study to optimise the gain of the PID controller. Based on the cost function, the DLFCO algorithm will adjust the gain. The root mean square cost function is used to optimise the PID controller (RMSE). The gains of the PID controller are shown in Eq. 23 and the cost function which needs to minimise is RMSE shown in Eq. 24.

$$variables = [K_p, K_i, K_d] \quad (23)$$

$$RMSE = \sqrt{(\sum_{t=0}^{T}(V_{out} - V_{ref})^2)/T)} \quad (24)$$

where V_{ref} is the reference voltage calculated by the machine-learning algorithm against the operating circumstances and V_{out} is the terminal voltage of PV modules. The PID gains K_p, K_i,and K_d which are initially randomly initialized inside the solution space. The cost function's value is examined, and the DLFCO algorithm is used to update the values of K_p,K_i,and K_d. The procedure is repeated until the cutoff requirements have been reached [14]. The PID gains are also adjusted using the DLFCO method. Following the DLFCO's successful PID training, gains are K_p=3.07·$10^{(-3)}$, K_i=0.89, and K_d=0. The PID test run's RMSE was achieved at 0.113.

IV. Results and Discussion

A. Simulation Setup

The simulation set up of the proposed model in a block diagram is shown in Fig. 6. The setup is divided into three main blocks. The ML model generates the reference voltage depending upon the operating temperature and irradiance levels. The data driven ML model generates the V_{ref}. The set point is achieved by the learning V_{pv} to the V_{ref}. The output is enforced by the corresponding PID block and MOSFET driver circuit [15]. The Boost converter block provides the control for power transform from input to output. The fitness Eq. 24 for training and testing is calculated using iterative samples by sensors. The sample time is 0.001s. The PV module is TMC25 with P_{max} of 20-25W.

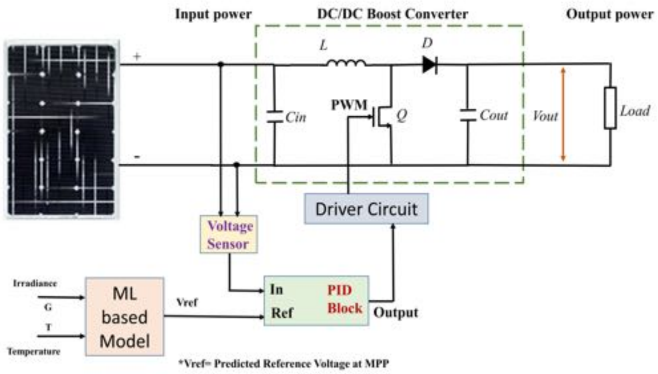

Fig. 6. Proposed Simulation Setup for Testing

B. Variation of Load

The load of the PV system varies with demand. The maximum power delivery requires an active impedance match between load and PV panels via DC converter. Fig. 7 shows the voltage transients corresponding to load variation. DLFCO is able to account for load variation well within 40ms i.e.

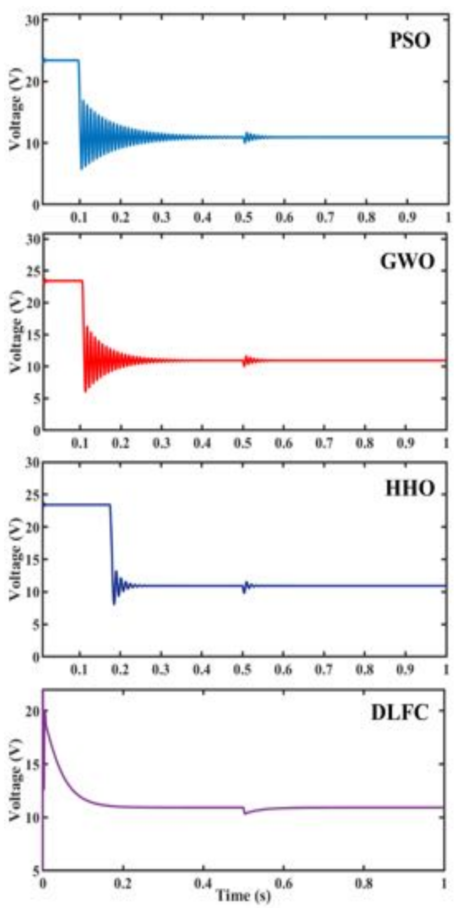

Fig. 7. Variation of Load

C. Variation of Environmental Conditions

The output of PV system is mainly impacted by irradiance and Temperature. The system initially operates at STC of 1000 W/m2 and 25ºC. At t=500ms, irradiance drops to 700 w/m2 with temperature rise to 30ºC. PSO exhibits large damping oscillation that take around 80ms to drop down with power tracking efficiency of less then 94%, GWO minimises the damping oscillations by 30% and slightly improvises tracking efficiency by 95.8%. The HHO exhibits the better performance still unable to compensate for the undesired fluctuation of voltage lowering the tracking efficiency by 97%. Proposed model successfully eliminates the damping oscillations with tracking efficiency of 99.9%.

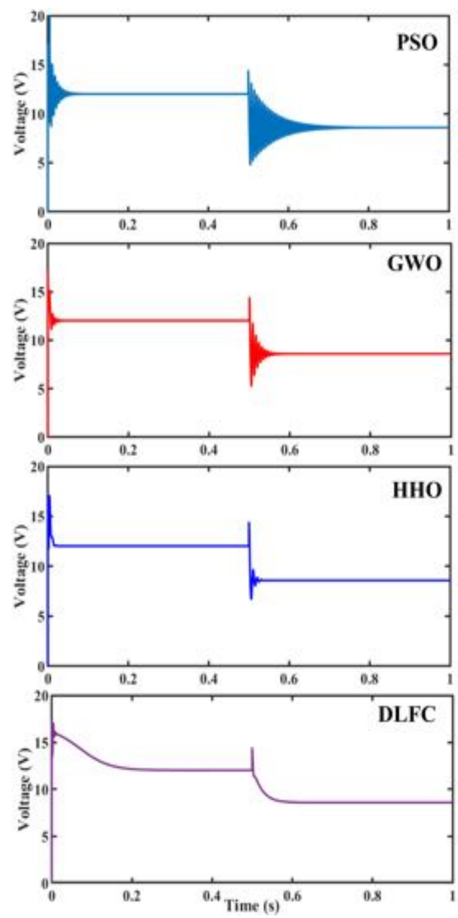

Fig. 8. Variation of Operating environmental conditions

D. Statistical Analysis

DLFCO is responsible for the greatest amount of energy harvesting, followed by HHO and GWO. PSO is the least effective method for achieving redundancy when used inside a hybrid architecture [16]. It is because of its long-lasting nature as well as its overall efficacy exhibited by Fig. 9. displays the results of the statistical study conducted on the recommended MPPT techniques. When evaluating the sensitivity of the techniques, relative error (RE), mean absolute error (MAE), and root mean square error (RMSE) are all useful metrics to employ. The RE, MAE, RMSE are shown in Eq. 25, 26 and 27, respectively.

$$RE = \frac{\sum_{i=1}^{n}(P_{pvi} - P_{pv})}{P_{pv}} * 100\% \tag{25}$$

$$MAE = \frac{\sum_{i=1}^{n}(P_{pvi} - P_{pv})}{n} \tag{26}$$

$$RMSE = \sqrt{\frac{\sum_{i=1}^{n}(P_{pvi} - P_{pv})^2}{P_{pv}}} \tag{27}$$

where $\mathrm{P_{pvi}}$ denotes the output power in the $\mathrm{i^{th}}$ iteration, $\mathrm{P_{pv}}$ illustrates the maximum output power of the PV system, n shows the total runs. The proposed technique achieves smaller RE and MAE than GRNN-HHO, GRNN-GWO and GRNN-PSO as shown in Fig.9.

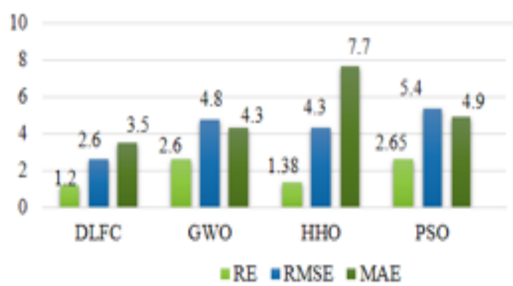

Fig. 9. Graphical presentation of Statistical analysis

V. Conclusion

This article provided a novel application of the Proportional-Integral-Derivative (PID) controller for Maximum Power Point Tracking (MPPT) of Photovoltaic System (PV) system. Dynamic Levy flight function is utilised in cognition with Fused champed algorithm (DLFCO) to improvise the classical parameters of PID. Moreover, the DLFCO algorithms is mathematically modelled to minimise the limitations of existing hybrid MPPT control. A comparison is made against the classical Particle Swarm Optimisation (PSO), Grey Wolf Optimiser (GWO), and recently developed HHO algorithms. The Machine Learning core is composed of General Regression Neural Network (GRNN) is altered with DLFCO. The proposed mechanism minimises the overshoot, ripples and settling time for MPPT control action. GRNN-DLFCO segregates the optimum parameters of PID. Online control-loops can also be used to manage the control signal of a DC Boost converter in order to reduce unwanted oscillations in the output power to the load when input circumstances and load vary.

For future endeavors, the stability of output voltage using the DLFCO as a control application instigates useful application in HVDC power transmission for fault detection.

Acknowledgment

This work is supported by the Top Research Centre Mechatronics (TRCM), Collaborative robots, University of Agder (UiA), Norway.

References

[1] J. Bao, J. Forbes, and P. McLellan, "Robust multiloop pid controller design: A successive semidefinite programming approach," *Industrial & engineering chemistry research*, vol. 38, no. 9, pp. 3407–3419, 1999.

[2] A. Khaled, H. Aboubakeur, B. Mohamed, and A. Nabil, "A fast mppt control technique using pid controller in a photovoltaic system," in *2018 International Conference on Applied Smart Systems (ICASS)*. IEEE, 2018, pp. 1–5.

[3] L. Chen, G. Chen, R. Wu, A. M. Lopes, J. Machado, and H. Niu, "Variable coefficient fractional-order pid controller and its application to a sepic device," *IET Control Theory & Applications*, vol. 14, no. 6, pp. 900–908, 2020.

[4] P. Jeba and A. Immanuel Selvakumar, "Fopid based mppt for photovoltaic system," *Energy sources, part A: Recovery, utilization, and environmental effects*, vol. 40, no. 13, pp. 1591–1603, 2018.

[5] K. Nisi, B. Nagaraj, and A. Agalya, "Tuning of a pid controller using evolutionary multi objective optimization methodologies and application to the pulp and paper industry," *International Journal of Machine Learning and Cybernetics*, vol. 10, no. 8, pp. 2015–2025, 2019.

[6] A. Kusmantoro, M. H. Purnomo, A. Priyadi, and V. L. B. Putri, "Fuzzy-pid controller on mppt pv to stabilize dc bus voltage," in *2019 International Conference on Technologies and Policies in Electric Power & Energy*. IEEE, 2019, pp. 1–6.

[7] M. T. Özdemir and D. Öztürk, "Comparative performance analysis of optimal pid parameters tuning based on the optics inspired optimization methods for automatic generation control," *Energies*, vol. 10, no. 12, p. 2134, 2017.

[8] A. Harrag and S. Messalti, "Ic-based variable step size neuro-fuzzy mppt improving pv system performances," *Energy Procedia*, vol. 157, pp. 362–374, 2019.

[9] A. Feroz Mirza, M. Mansoor, Q. Ling, M. I. Khan, and O. M. Aldossary, "Advanced variable step size incremental conductance mppt for a standalone pv system utilizing a ga-tuned pid controller," *Energies*, vol. 13, no. 16, p. 4153, 2020.

[10] R. H. Tan and L. Y. Hoo, "Dc-dc converter modeling and simulation using state space approach," in *2015 IEEE Conference on Energy Conversion (CENCON)*. IEEE, 2015, pp. 42–47.

[11] M. Khishe and M. R. Mosavi, "Chimp optimization algorithm," *Expert systems with applications*, vol. 149, p. 113338, 2020.

[12] S. K. Pattnayak, S. Choudhury, N. Nayak, D. Bagarty, and M. Biswabandhya, "Maximum power tracking & harmonic reduction on grid pv system using chaotic gravitational search algorithm based mppt controller," in *2020 International Conference on Computational Intelligence for Smart Power System and Sustainable Energy (CISPSSE)*. IEEE, 2020, pp. 1–6.

[13] A. F. Kamaruzaman, A. M. Zain, S. M. Yusuf, and A. Udin, "Levy flight algorithm for optimization problems-a literature review," *Applied mechanics and materials*, vol. 421, pp. 496–501, 2013.

[14] M. H. Zafar, N. M. Khan, M. Mansoor, A. F. Mirza, S. K. R. Moosavi, and F. Sanfilippo, "Adaptive ml-based technique for renewable energy system power forecasting in hybrid pv-wind farms power conversion systems," *Energy Conversion and Management*, vol. 258, p. 115564, 2022.

[15] M. K. Khan, M. H. Zafar, M. Mansoor, A. F. Mirza, U. A. Khan, and N. M. Khan, "Green energy extraction for sustainable development: A novel mppt technique for hybrid pv-teg system," *Sustainable Energy Technologies and Assessments*, vol. 53, p. 102388, 2022.

[16] M. Mansoor, Q. Ling, and M. H. Zafar, "Short term wind power prediction using feedforward neural network (fnn) trained by a novel sine-cosine fused chimp optimization algorithm (schoa)," in *2022 5th International Conference on Energy Conservation and Efficiency (ICECE)*. IEEE, 2022, pp. 1–6.